Laser Flash Induced Electron Transfer in P450cam Monooxygenase: Putidaredoxin Reductase−Putidaredoxin Interaction†

Irina F. Sevrioukova,*,‡ James T. Hazzard,§ Gordon Tollin,§ and Thomas L. Poulos‡,||

Departments of Molecular Biology and Biochemistry and of Physiology and Biophysics, and Program in Macromolecular Structure, University of California, Irvine, California 92612-3900, and Department of Biochemistry and Molecular Biophysics, University of Arizona, Tucson, Arizona 85721

Received April 30, 2001; Revised Manuscript Received July 9, 2001

ABSTRACT: The P450cam monooxygenase from *Pseudomonas putida* consists of three redox proteins: NADH−putidaredoxin reductase (Pdr), putidaredoxin (Pdx), and cytochrome P450cam. The redox properties of the FAD-containing Pdr and the mechanism of Pdr−Pdx complex formation are the least studied aspects of this system. We have utilized laser flash photolysis techniques to produce the one-electron-reduced species of Pdr, to characterize its spectral and electron-transferring properties, and to investigate the mechanism of its interaction with Pdx. Upon flash-induced reduction by 5-deazariboflavin semiquinone, the flavoprotein forms a blue neutral FAD semiquinone (FADH•). The FAD semiquinone was unstable and partially disproportionated into fully oxidized and fully reduced flavin. The rate of FADH• decay was dependent on ionic strength and NAD^+. In the mixture of Pdr and Pdx, where the flavoprotein was present in excess, electron transfer (ET) from FADH• to the iron−sulfur cluster was observed. The Pdr-to-Pdx ET rates were maximal at an ionic strength of 0.35 where a kinetic dissociation constant (K_d) for the transient Pdr−Pdx complex and a limiting k_{obs} value were equal to 5 μM and 226 s^{-1}, respectively. This indicates that FADH• is a kinetically significant intermediate in the turnover of P450cam monooxygenase. Transient kinetics as a function of ionic strength suggest that, in contrast to the Pdx−P450cam redox couple where complex formation is predominantly electrostatic, the Pdx−Pdr association is driven by nonelectrostatic interactions.

The soluble P450cam[1] monooxygenase from *Pseudomonas putida* consists of cytochrome P450cam, CYP101 (45 kDa), an iron−sulfur protein putidaredoxin (Pdx, 11.5 kDa), and a FAD-containing NADH−putidaredoxin reductase (Pdr, 45.6 kDa). The system catalyzes the regio- and stereospecific hydroxylation of camphor consuming two electrons and molecular oxygen per reaction cycle (eq 1).

$$RH + O_2 + NADH + 2H^+ + 2e \rightarrow ROH + NAD^+ + H_2O \quad (1)$$

There are three distinct electron-transfer (ET) processes required in the overall cycle. First, Pdr accepts 2 reducing equiv from NADH. Second, a single electron is transferred from Pdr to the $(Fe-S)_2$ cluster in Pdx. Third, the reduced Pdx delivers its electron to the heme iron of P450cam. Of these, the ET reaction between P450cam and Pdx has been thoroughly studied [for review, see ref (*1*)]. Chemical modification and mutagenesis experiments have provided information concerning residues of P450cam and Pdx that might be involved in the protein−protein interaction and ET (*2*−*7*). In addition, a structure-based model for a P450cam−Pdx complex has been proposed (*8*) based on the crystal structure of P450cam (*9*) and the NMR structure of Pdx (*10*).

Pdr is the least studied protein in the P450cam monooxygenase system. Although some of its redox properties have been analyzed (*11*, *12*), the required one-electron-reduced intermediate of Pdr involved in catalysis has not been identified. Moreover, little is known about the ET reaction between Pdx and Pdr. The available data are contradictory and show involvement of either electrostatic (*11*), both hydrophobic and electrostatic (*2*), or predominantly hydrophobic components (*13*) and steric factors (*7*) in the association between Pdr and Pdx. The direct Pdr−Pdx interaction has proven to be difficult to study due to spectral overlap between FAD and the $(Fe-S)_2$ center. As a result, the Pdr-to-Pdx ET reaction has been investigated only indirectly by following the reduction of cytochrome *c* by reduced Pdx (*7*, *14*).

A more detailed understanding of Pdr and the Pdr−Pdx interaction has implications beyond the P450cam monooxygenase system. Pdr exhibits significant structural similarity

† This work was supported by NIH Grants GM19749 (I.F.S.), GM33688 (T.L.P.), and DK15057 (G.T.).

* To whom correspondence should be addressed. Tel.: 949-824-4322. Fax: 949-824-3280. E-mail: sevrioui@uci.edu.

‡ Department of Molecular Biology and Biochemistry, University of California.

§ Department of Biochemistry and Molecular Biophysics, University of Arizona.

|| Department of Physiology and Biophysics, University of California.

[1] Abbreviations: P450cam, cytochrome P450 CYP101 isolated from *Pseudomonas putida*; Pdx, putidaredoxin; Pdr, putidaredoxin reductase; ET, electron transfer; dRF, 5-deazariboflavin; dRFH•, 5-deazariboflavin semiquinone; FADH•, blue neutral FAD semiquinone; ONFR, an oxygenase-coupled NADH-dependent ferredoxin reductase; BphA4, an ONFR component in biphenyl dioxygenase from *Pseudomonas putida*; Adx, adrenodoxin; Adr, NADPH−adrenodoxin reductase.

10.1021/bi010874d CCC: $20.00
Published on Web 08/10/2001

to the bacterial oxygenase-coupled NADH-dependent ferredoxin reductases (ONFR), the proteins that adopt the same fold as enzymes of the glutathione reductase family but not that of $NADP^+$−ferredoxin reductases (*15*). Therefore, ONFR−redox partner complexes, in general, and the Pdx−Pdr pair, in particular, may not be typical of this well-studied class of complex-forming flavoprotein/iron−sulfur protein pairs (*16, 17*). The ONFR's have drawn more attention recently after their homologue was found in mammalian mitochondria. The protein has been identified as an apoptosis-inducing factor, a bifunctional enzyme with an electron acceptor/donor and an apoptogenic function (*18*). The reactions catalyzed by ONFR's have not been characterized. Thus, elucidation of the electron-transferring properties of Pdr may be useful for better understanding how this group of flavoproteins functions.

Some of the advantages of the laser flash photolysis technique for determining the spectral and kinetic behavior of one-electron-reduction products of flavoproteins, as well as for measuring transient kinetics of intracomplex ET for a number of protein−protein systems, have been demonstrated [for review, see refs (*19*) and (*20*)]. In the present study, we have adapted this method for studying the P450cam monooxygenase ET reactions. This has enabled the first characterization of the one-electron-reduced species of Pdr and investigation of its interaction with Pdx. In addition, a reconstituted system was developed to monitor the ET reaction from laser flash reduced Pdx to P450cam to measure and compare kinetic parameters for the ET reactions between the two redox pairs in P450cam monooxygenase under similar conditions.

EXPERIMENTAL PROCEDURES

Materials. Pdx and P450cam expression plasmids were kindly provided by Dr. S. Sligar (University of Illinois, Urbana, IL). Recombinant proteins were expressed in *E. coli* and purified as described previously (*21*). Purified P450cam and Pdx used in the experiments had ratios of A_{392}/A_{280} and A_{412}/A_{280} greater than 1.4 and 0.9, respectively. The pET-Pdr plasmid for expression of Pdr was received from Dr. P. R. Ortiz de Montellano (University of California, San Francisco, CA).

Expression and Purification of Pdr. Expression and purification of Pdr was carried out according to the procedure developed by Laura Koo (L. Koo and P. R. Ortiz de Montellano, unpublished results) with a few modifications. The pET-Pdr plasmid was transformed into the BL21 strain of *E. coli*. Cells were grown in TB medium supplemented with ampicillin (100 mg/L) to $A_{600} = 0.9$ at 37 °C. The temperature then was lowered to 30 °C, and isopropyl-1-thio-β-D-galactopyranoside (1 mM) was added. The culture was allowed to grow for 24 h. The cells collected by centrifugation were resuspended in 20 mM potassium phosphate buffer, pH 7.5, 0.1 mM phenylmethylsulfonyl fluoride (buffer A) and treated with lysozyme (200 mg/L). After stirring at 4 °C for 1 h, the suspension was sonicated using a Branson sonicator (medium power output) until the viscous consistency due to the nucleic acids was disrupted (~2 min). The soluble fraction after centrifugation at 100000*g* for 30 min was subjected to ammonium sulfate precipitation. The fraction that precipitated between 35 and 70% saturated ammonium sulfate was dialyzed against buffer A. After precipitated proteins were removed from the dialysate by centrifugation, it was loaded on a 150 mL Q-Sepharose ion-exchange column (Pharmacia Biotech) previously equilibrated with buffer A. The column was extensively washed first with buffer A and then with buffer A containing 0.1 M KCl. Pdr was eluted with a 100−400 mM linear gradient of KCl. Fractions with the highest A_{455}/A_{280} ratios were combined, concentrated, and loaded on a 500 mL Sephacryl S-100 HR gel filtration column equilibrated with 50 mM potassium phosphate buffer, pH 7.5, 0.1 mM phenylmethylsulfonyl fluoride. Pdr was purified to homogeneity on a 20 mL phenyl-Sepharose column (Pharmacia Biotech) using a linear 30−0% ammonium sulfate gradient in buffer A. The protein with a ratio of A_{280}/A_{455} less than 7.0 was used in the experiments.

Spectroscopic Studies. All UV−visible spectroscopy was performed using a Cary 3 spectrometer. P450 content was measured by a reduced CO-difference spectrum using $\epsilon_{450\ nm} = 91\ mM^{-1}\ cm^{-1}$ (*22*). Concentrations of Pdx and Pdr were calculated using extinction coefficients of 10.4 $mM^{-1}\ cm^{-1}$ at 455 nm and 11.0 $mM^{-1}\ cm^{-1}$ at 412 nm, respectively (*21*).

Laser Flash Photolysis Experiments. Laser flash photolysis experiments were performed anaerobically at room temperature as described elsewhere (*19*). The technique involves the in situ generation of a strong reductant, dRF semiquinone ($dRFH^\bullet$), through the excitation of dRF by a laser pulse, followed by rapid bimolecular reduction of the protein's redox center by $dRFH^\bullet$. If a complex of redox partners is present in the solution and one partner is reduced preferentially, the rate of intermolecular ET can subsequently be followed spectroscopically. Potassium phosphate buffer solutions, pH 6.0, 7.0, or 8.0, contained 100 μM dRF and 2 mM semicarbazide as a sacrificial electron donor. The absence of oxygen was monitored by the amplitude and decay of the $dRFH^\bullet$ transient signal obtained at 500 nm upon laser excitation of the reaction mixture prior to addition of the enzyme(s). To maintain anaerobiosis, all aliquots of added protein or substrate were subjected to a flow of oxygen-free argon prior to mixing with the bulk reaction solution. Ionic strength was adjusted by adding aliquots of 1 M potassium phosphate buffer. The protein concentration was always larger than the concentration of $dRFH^\bullet$ generated by the laser flash, so that pseudo-first-order conditions applied and no more than a single electron could enter each protein molecule. Transient kinetic data were collected using a Tektronix TDS 410A digitizing oscilloscope and analyzed on a PC using Igor Pro (WaveMetrics, Inc.).

Enzyme Assays. Cytochrome P450cam hydroxylation activity was determined in the complete system of three proteins by measuring rates of substrate-dependent NADH oxidation and O_2 consumption at 20 °C. The reaction mixture of 1.4 mL contained 0.5 μM Pdr, 5 μM Pdx, and 0.5 μM P450cam in phosphate buffer, pH 7.5. The rate of NADH oxidation was measured by monitoring the absorbance change at 340 nm using $\epsilon = 6.22\ mM^{-1}\ cm^{-1}$. The reaction was initiated by addition of NADH (300 μM final concentration). The rate of substrate-dependent NADH oxidation was assayed under the same conditions but in the presence of 200 μM camphor and was calculated as the difference

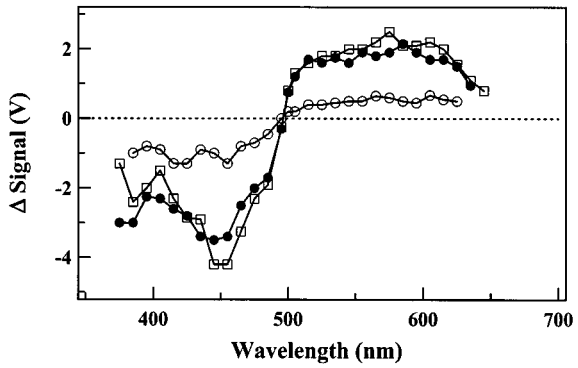

FIGURE 1: Time-resolved laser-flash photolysis difference spectra for the reduction of Pdr by dRF semiquinone. The reaction solution contained 100 mM phosphate buffer, pH 6.0 (○), 7.0 (□), or 8.0 (●), 100 μM dRF, 2 mM semicarbazide, and 40 μM protein.

between the measured rate and the rate of nonspecific NADH oxidation in the absence of camphor. Oxygen consumption was measured with a Hansatech Oxytherm (Norfolk, England) under conditions identical to those described for the determination of NADH oxidation rates.

RESULTS

One-Electron Reduction of Pdr. Upon laser flash photolysis of dRF solutions in the presence of a sacrificial electron donor (e.g., semicarbazide) and in the absence of other electron-transfer agents, the dRFH$^\bullet$ produced by the laser flash decays by disproportionation (*23*). In the presence of an electron-accepting protein which can react with dRFH$^\bullet$, one can obtain a time-resolved one-electron-reduced minus oxidized difference spectrum for that protein by monitoring transient signals at various wavelengths. Figure 1 shows the kinetic redox difference spectrum obtained 10 ms after reduction of Pdr by dRFH$^\bullet$. An absorption minimum was observed at 455 nm due to FAD reduction, while a broad absorption maximum was observed in the 520−620 nm region. These absorbance changes are similar to those observed during formation of the blue neutral flavin semiquinone, FADH$^\bullet$ (*24*). The difference spectrum was not affected by pH in the 6.0−8.0 range. Smaller signal changes observed at pH 6.0 were due to instability and partial precipitation of Pdr. Since the recombinant enzyme was found to be more stable and active at pH 8.0, further experiments described below were carried out at this pH.

Kinetic traces obtained at 455 and 585 nm, corresponding to maximal absorbance changes observed in the redox difference spectrum (Figure 1), were chosen to follow the extent of FAD reduction and to monitor the formation and decay of the FAD semiquinone (FADH$^\bullet$), respectively (Figure 2). The reaction of dRFH$^\bullet$ with Pdr obeys pseudo-first-order kinetics since less than 1 μM dRFH$^\bullet$ is generated in a solution containing 10−40 μM Pdr. The plot of k_{obs} versus Pdr concentration for the reaction of Pdr with dRFH$^\bullet$ in 100 mM phosphate buffer is hyperbolic (Figure 3), suggesting that dRFH$^\bullet$ forms a complex with Pdr prior to electron transfer. A hyperbolic fit gives a limiting k_{obs} value of 1.3×10^4 s^{-1} extrapolated to infinite [Pdr] and a dissociation constant, K_d, of 10 μM for the interaction of dRFH$^\bullet$ with Pdr. An apparent bimolecular rate constant for the reaction, k_{app}, determined from the initial slope of the plot in Figure 3, was found to be 7.2×10^8 M^{-1} s^{-1}.

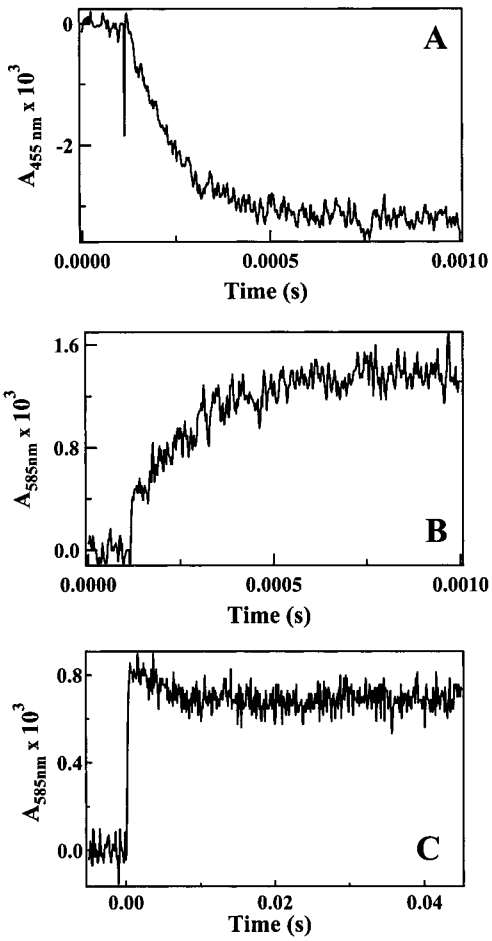

FIGURE 2: Absorption changes after laser flash excitation of a dRF/semicarbazide solution containing Pdr. (A) Transients obtained at 455 nm to observe FAD reduction ($\epsilon_{445nm} = 10.4$ mM^{-1} cm^{-1}). (B and C) Transients obtained at 585 nm to follow blue, neutral FAD semiquinone formation and disproportionation ($\epsilon_{585nm} = 5$ mM^{-1} cm^{-1}). Solutions contained 100 μM dRF, 2 mM semicarbazide, and 30 μM protein in 100 mM phosphate buffer, pH 8.0.

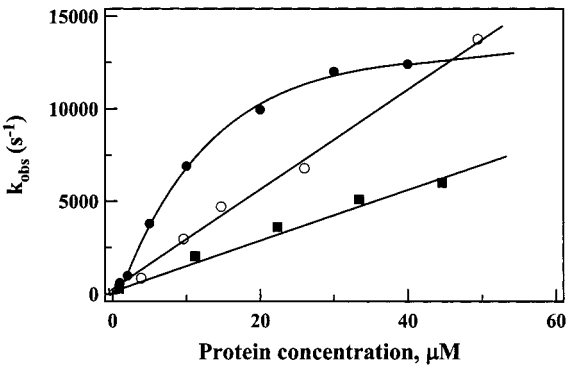

FIGURE 3: Second-order plots for the reduction of Pdr (●), Pdx (○), and P450cam (■) by dRF semiquinone. Kinetics were monitored at 455, 457, and 443 nm, respectively. The reaction solution contained 100 μM dRF and 2 mM semicarbazide in 100 mM phosphate buffer, pH 8.0. Camphor (400 μM) was present in the reaction mixture containing P450cam.

According to the amplitude of the absorbance decrease at 585 nm (Figure 2C), approximately one-fourth of the Pdr semiquinone disproportionated to form the fully oxidized and fully reduced FAD whereas three-fourths of the FADH$^\bullet$ was stable within the studied time interval. The reason for this effect is not clear. The observed rate constant for the

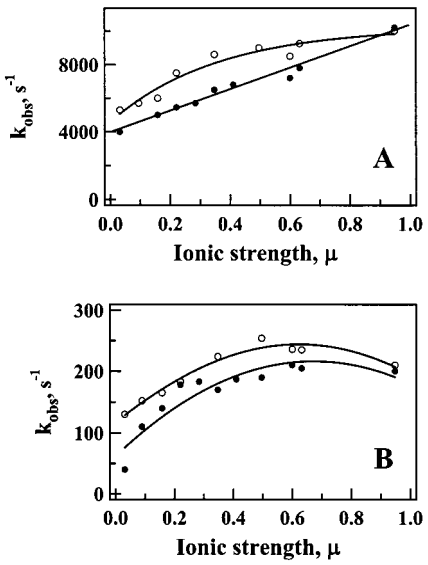

FIGURE 4: Effect of ionic strength and NAD^+ on Pdr FAD semiquinone formation (A) and disproportionation (B). Reactions were followed at 585 nm. The reaction mixture contained 100 μM dRF, 2 mM semicarbazide, 30 μM Pdr, and different concentrations of potassium phosphate buffer, pH 8.0, in the absence (●) or presence (○) of 200 μM NAD^+.

disproportionation reaction was dependent on Pdr concentration. The plot of k_{obs} for the reaction of $FADH^\bullet$ disproportionation versus [Pdr] measured in 100 mM phosphate buffer was hyperbolic with the limiting value of k_{obs} for the $FADH^\bullet$ disproportionation reaction equal to 256 s^{-1} (data not shown).

The reactions of FAD semiquinone formation and disproportionation were affected by ionic strength and by the presence of NAD^+ in the reaction mixture. An increase of ionic strength from 0.032 to 0.96 resulted in a linear 2.5-fold increase in the rate constant of Pdr reduction by $dRFH^\bullet$, indicating that the interaction between $dRFH^\bullet$ and the flavoprotein is primarily nonelectrostatic (Figure 4A). However, since the $dRFH^\bullet$ is zwitterionic owing to delocalization of the unpaired electron, the small increase in k_{obs} with increasing I may reflect a weak electrostatic repulsion of $dRFH^\bullet$ by the reduction site on Pdr. The rate constant of the reaction of $FADH^\bullet$ disproportionation was increased 5-fold with an increase of ionic strength from 0.032 to 0.96 and was maximal at $I = 0.6$ (Figure 4B). The effect of ionic strength on FAD semiquinone disproportionation was more pronounced than on the preceding reaction. This suggests that interaction between one-electron-reduced molecules of Pdr, facilitated at an intermediate ionic strength, is primarily driven by nonelectrostatic forces and/or might be hindered by electrostatic repulsion at low ionic strength.

When NAD^+ was present in the reaction mixture, both FAD reduction and $FADH^\bullet$ disproportionation reactions occurred more rapidly over the entire range of ionic strength studied (Figure 4). NAD^+, thus, plays a dual role. First, it facilitates reduction of Pdr by $dRFH^\bullet$, thereby facilitating $FADH^\bullet$ production. Second, NAD^+ destabilizes the FAD semiquinone by promoting the $FADH^\bullet$ disproportionation reaction and formation of the fully reduced Pdr. It should be noted that the presence of NAD^+ in the reaction mixture interfered with the production of $dRFH^\bullet$ by the laser pulse. The amount of dRF semiquinone produced was significantly lower and the $dRFH^\bullet$ decay time was longer than the same

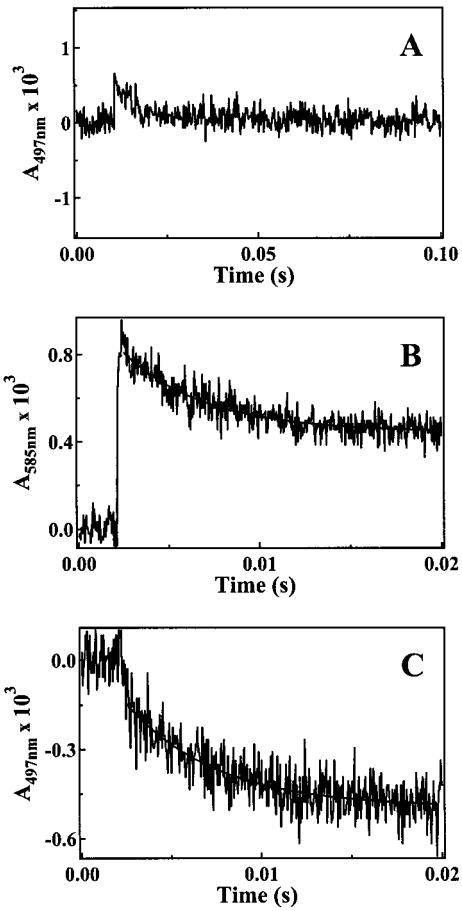

FIGURE 5: Transient kinetics observed after laser flash excitation of a dRF/semicarbazide solution containing Pdr in the absence and presence of Pdx. (A) Transients obtained at 497 nm, an isosbestic point for the reduced and oxidized forms of Pdr, in the absence of Pdx. (B and C) Transients obtained at 585 and 497 nm to follow FAD semiquinone disproportionation and Pdx reduction, respectively ($\epsilon_{585nm} = 5$ mM^{-1} cm^{-1}, $\epsilon_{497nm} = 6.7$ mM^{-1} cm^{-1}). Solutions contained 100 μM dRF, 2 mM semicarbazide, and either 30 μM Pdr (A) or 30 μM Pdr and 20 μM Pdx (B and C) in 100 mM phosphate buffer, pH 8.0. The smooth lines represent single-exponential fits giving rate constants of 226 (B) and 200 s^{-1} (C).

parameters measured in the absence of NAD^+ (data not shown), most likely due to formation of a charge-transfer complex between reduced dRF and oxidized NAD^+. Due to this complication, NAD^+ was not used for studying the ET reactions in the reaction system consisting of a mixture of Pdr and Pdx.

Laser Flash-Induced Pdr-to-Pdx Electron Transfer. $dRFH^\bullet$ also is able to reduce Pdx, and the plot of k_{obs} versus Pdx concentration for the reaction of Pdx with $dRFH^\bullet$ is linear (Figure 3) with a second-order rate constant of 2.4×10^8 M^{-1} s^{-1}. This value is 3-fold lower than the apparent bimolecular rate constant for the reduction of Pdr by $dRFH^\bullet$. Although there is a high degree of spectral overlap between Pdr and Pdx, it was possible to measure interprotein ET from Pdr to Pdx because, as noted above, Pdr was reduced faster by $dRFH^\bullet$ and it was present at higher concentration relative to that of Pdx. For the Pdr−Pdx mixture, the reaction could be monitored by following the formation/disappearance of the FAD semiquinone at 585 nm, and by following reduction of the Pdx $(Fe-S)_2$ center at 497 nm, an isosbestic point in the one-electron redox difference spectrum of Pdr (Figures 1 and 5A). The rate constant for direct reduction of the Pdr

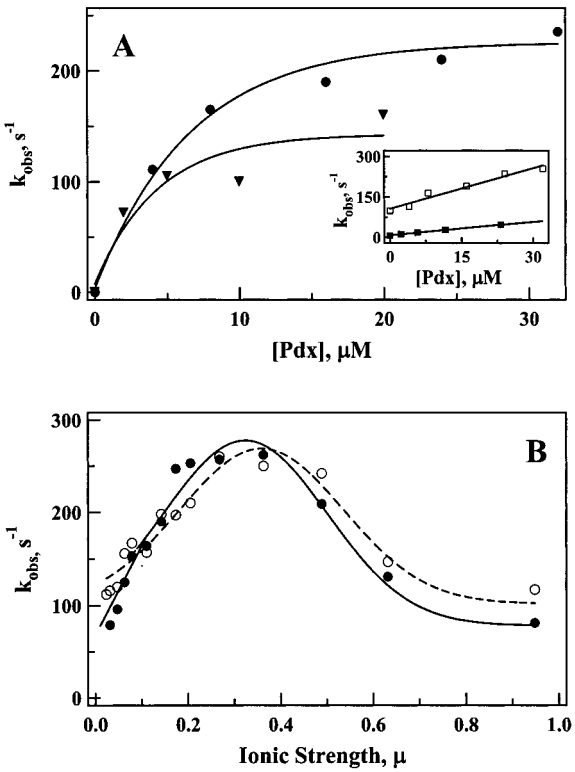

FIGURE 6: Dependence of observed rate constants for the reduction of Pdx by Pdr on Pdx concentration and ionic strength. (A) The rate constants were measured at 497 (●, ▼) and 585 nm (■, □) at ionic strengths of 0.032 (▼, ■) and 0.32 (●, □). The reaction mixture contained 100 μM dRF, 2 mM semicarbazide, 40 μM Pdr, and different concentrations of Pdx in phosphate buffer, pH 8.0. The solid lines represent fits to the data points assuming a two-step mechanism of binding followed by ET. (B) The rate constants were measured at 497 (●) and 585 nm (○) in phosphate buffer, pH 8.0, containing 100 μM dRF, 2 mM semicarbazide, 30 μM Pdr, and 20 μM Pdx. The ionic strength was adjusted with potassium phosphate, pH 8.0.

FAD by dRFH$^{\bullet}$ in the presence of Pdx was similar to that for the free protein under all conditions studied (data not shown). This suggests that there is no steric hindrance or flavin redox potential change of Pdr in the presence of Pdx.

In the presence of Pdx, the absorbance decay at 585 nm, corresponding to FADH$^{\bullet}$ oxidation, was dependent on Pdx concentration and occurred on the same time scale as reduction of Pdx monitored at 497 nm. Reactions monitored at both wavelengths were monophasic (Figure 5B,C). As the amount of Pdx relative to Pdr was increased, the signals at both wavelengths increased correspondingly. The rate of Pdx reduction in the presence of Pdr was an order of magnitude slower than the rate of Pdx reduction by dRFH$^{\bullet}$. It is important to point out that during this slow phase dRFH$^{\bullet}$ is not present in solution any more. The radical exists only for a few milliseconds after laser pulse [$t_{1/2} = 0.5$ ms (*20*)] and becomes oxidized during the fast phase of the reaction after transferring a reducing equivalent to the protein present in excess in the reaction mixture (Pdr). This demonstrates that there was no direct reduction of Pdx by dRFH$^{\bullet}$ in the Pdr−Pdx mixture and that Pdx receives electrons from the FAD semiquinone of Pdr.

The dependence of signal changes at 497 and 585 nm on Pdx concentration is shown in Figure 6A. Saturation kinetics were observed for the rate constants measured at 497 nm,

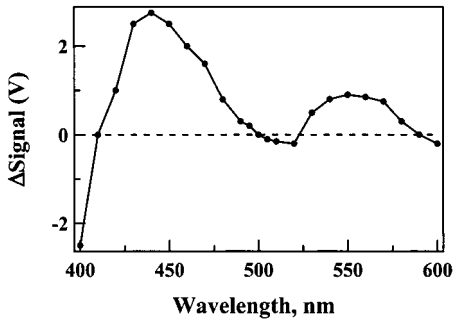

FIGURE 7: Time-resolved laser-flash photolysis difference spectrum for the reduction of P450cam by dRF semiquinone. The reaction solution contained 100 mM phosphate buffer, pH 8.0, 100 μM dRF, 2 mM semicarbazide, 20 μM hemoprotein, and 400 μM camphor.

whereas the signal change at 585 nm, reflecting both disproportionation between one-electron-reduced Pdr molecules and the Pdr-to-Pdx ET, increased linearly with an increase of [Pdx]. The interprotein ET was affected by ionic strength. A 10-fold increase of ionic strength resulted in an increase in the limiting value of k_{obs} from 140 to 226 s^{-1} and a slight increase of the K_d for ET within the transient Pdr−Pdx complex from 3.5 to 5 μM (Figure 6A). As seen from the data in Figure 6B, the effect of ionic strength on the Pdr−Pdx ET was biphasic with the optimal ionic strength for the ET reaction between one-electron-reduced Pdr and Pdx being $I \approx 0.35$. The small change of K_d over a wide range of ionic strength and the biphasic character of ionic strength on the Pdr−Pdx ET indicate that ET complex formation between these redox partners is an intricate process and involves both electrostatic and hydrophobic interactions. The relatively high ionic strength required for optimal Pdr-to-Pdx ET suggests that nonelectrostatic forces predominate in the interprotein complex formation.

Laser Flash-Induced Pdx-to-P450cam Electron Transfer. Similar to Pdr and Pdx, substrate-bound P450cam could be separately reduced by a laser flash in the presence of dRF and semicarbazide. The dRFH$^{\bullet}$-to-P450cam ET was observed both in the absence and in the presence of carbon monoxide. However, in the presence of CO, the rate constants measured at 450 nm, an absorbance maximum for reduced CO-bound P450, were more than an order of magnitude smaller than those determined at 522 nm, an isosbestic point for reduced and reduced CO-bound P450cam (data not shown). This indicates that carbon monoxide binding to the ferrous substrate-bound heme iron was greatly hindered in our system. We speculate that molecules of dRF and/or semicarbazide present in the reaction mixture are capable of penetrating into the active site of P450cam and interfere with CO binding. To avoid this complication, carbon monoxide was not present in the experiments described below. The redox difference spectrum of substrate-bound P450cam obtained in the absence of CO at 10 ms after the pulse (Figure 7), as expected, had maxima at 443 and 553 nm. The second-order rate constant for the reduction of P450cam by dRFH$^{\bullet}$ measured at 443 nm is 1.3×10^8 M^{-1} s^{-1} as demonstrated by the concentration dependence data (Figure 3).

Due to spectral overlap between Pdx and P450cam and a considerably higher heme absorption in the Soret region, Pdx reduction in the P450cam−Pdx mixture was monitored at 500 nm, an isosbestic point for the oxidized and reduced

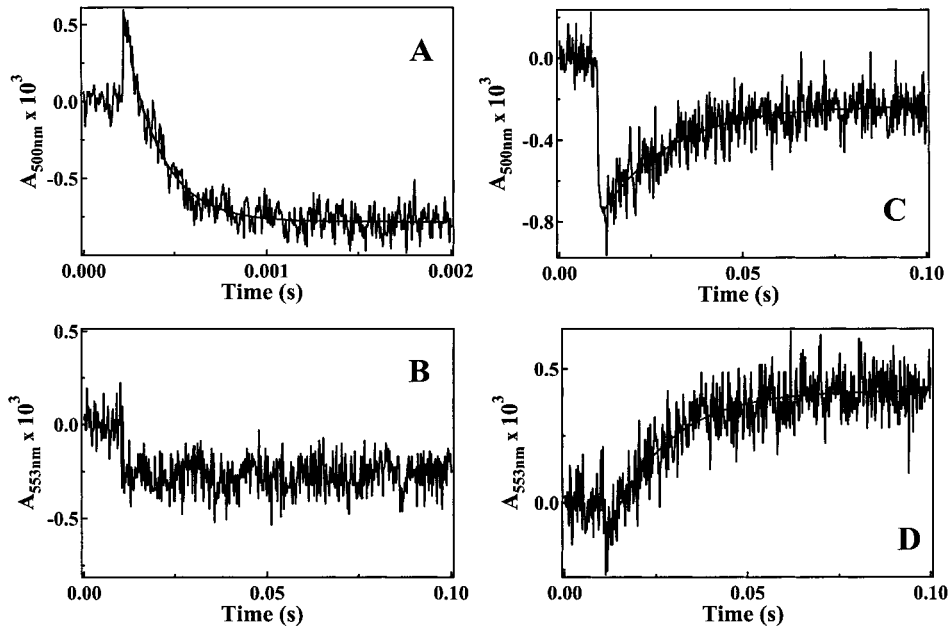

FIGURE 8: Transient kinetics observed after laser flash excitation of a dRF/semicarbazide solution containing Pdx (A and B) and its mixture with P450cam (C and D). (A and B) Transients obtained at 500 and 553 nm, respectively, to monitor Pdx reduction. Solutions contained 100 μM dRF, 2 mM semicarbazide, and 20 μM Pdx in 10 mM phosphate buffer, pH 8.0. (B and C) Transients obtained at 500 nm, an isosbestic point for the reduced and oxidized forms of P450cam, to follow Pdx reoxidation (ϵ_{500nm} = 6.6 mM^{-1} cm^{-1}), and 553 nm to follow P450cam reduction (ϵ_{553nm} = 14 mM^{-1} cm^{-1}). Solutions contained 100 μM dRF, 2 mM semicarbazide, 400 μM camphor, 20 μM Pdx, and 4 μM P450cam in 10 mM phosphate buffer, pH 8.0. The smooth lines represent single-exponential fits giving rate constants of 5500 (A), 55 (C), and 60 s^{-1} (D).

heme (Figure 7). P450cam reduction was followed at 553 nm. In the absence of P450cam, the absorbance at 500 and 553 nm decayed below the preflash baseline, consistent with the loss of absorbance due to $(Fe-S)_2$ cluster reduction in Pdx. There was no Pdx reoxidation within 100 ms after the laser flash (Figure 8 A,B).

In the mixture of the two proteins where Pdx was present in excess of P450cam, laser flash photolysis resulted in an initial fast decrease in absorbance in the 500−553 nm region followed by a subsequent slower absorbance increase at both wavelengths within a 100 ms time interval (Figure 8C,D). The spectral changes indicate that Pdx was preferentially reduced by dRFH$^\bullet$ and then reoxidized by P450. The rate of reduction of Pdx by dRFH$^\bullet$ was not altered in the presence of P450cam, indicating that P450cam does not hinder access of dRFH$^\bullet$ to the Pdx $(Fe-S)_2$ center. The rate constants for P450cam reduction were comparable with those for Pdx reoxidation and were 2 orders of magnitude lower than those for direct reduction of the hemoprotein by dRFH$^\bullet$. These data, and the fact that dRF radical has a lifetime of only a few milliseconds and is getting oxidized by the protein present in excess (Pdx) during the fast phase of the reaction, show that P450cam received electrons from Pdx and not directly from dRFH$^\bullet$.

The dependence of k_{obs} for the Pdx−P450cam ET reaction versus [P450cam] at two different ionic strengths is shown in Figure 9A. The hyperbolic plots give limiting values of k_{obs} for the ET reaction of 112 and 74 s^{-1} and a K_d value of 2 μM for the formation of the transient Pdx−P450cam complex at an ionic strength of 0.032 and 0.32, respectively. Again, a biphasic ionic strength dependence for interprotein ET was obtained, and k_{obs} was maximal at I = 0.05 (Figure 9B). At ionic strengths higher than 0.5, the ET rate constant did not change significantly and was equal to 16 s^{-1}. As

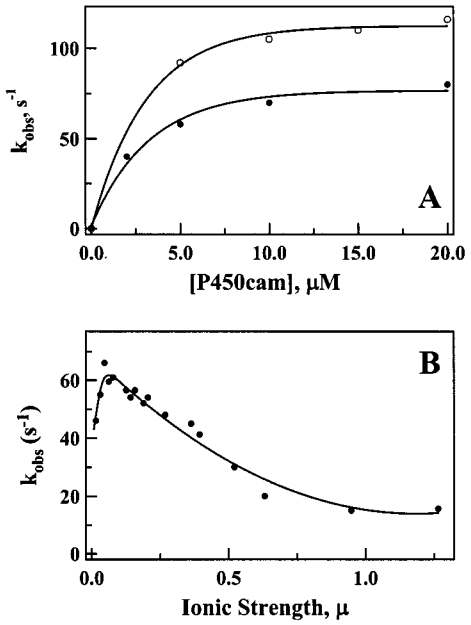

FIGURE 9: Plots of k_{obs} for the ET reaction from Pdx to P450cam versus P450cam concentration (A) and ionic strength (B). (A) The rate constants were measured at ionic strengths of 0.032 (○) and 0.32 (●) in phosphate buffer, pH 8.0, containing 100 μM dRF, 2 mM semicarbazide, 400 μM camphor, 40 μM Pdx, and different concentrations of P450cam. (B) The reaction mixture contained 100 μM dRF, 2 mM semicarbazide, 400 μM camphor, 20 μM Pdx, and 4 μM P450cam in phosphate buffer, pH 8.0. The ionic strength was adjusted with potassium phosphate, pH 8.0.

noted above, this type of dependence is indicative of an involvement of both electrostatic and hydrophobic interactions in Pdx−P450cam complex formation. However, compared to the Pdr−Pdx couple, considerably lower ionic strength was required to reach an optimal intramolecular ET in the P450cam−Pdx complex. This suggests that an

electrostatic component is predominant in the complex formation between these redox partners.

DISCUSSION

One-Electron-Reduced Species of Pdr. The main purpose of this study was to probe in more detail the Pdr−Pdx reaction which, until now, has not been studied using flash photolysis methods. An important unknown in this system has been the nature of the one-electron-reduced FAD that must be part of the catalytic cycle. Oxidation of two-electron-reduced Pdr by a one-electron acceptor Pdx implies formation of a semioxidized flavin intermediate during the P450cam monooxygenase catalytic cycle. Due to instability of the semiquinone form of Pdr, the intermediate could not be detected and characterized by conventional spectrophotometric techniques (*11, 12*), and investigation of its interaction with Pdx was not possible. To overcome this problem, we used laser flash photolysis techniques to form the Pdr semiquinone and characterize its spectral and electron-transferring properties. Our results show that Pdr easily reacts with dRFH$^{\bullet}$ and, upon one-electron reduction, produces a blue neutral FAD semiquinone within the pH 6.0−8.0 range (Figure 2). FADH$^{\bullet}$, therefore, is an intermediate formed by Pdr under physiological conditions. We found that reduction of Pdr by dRFH$^{\bullet}$, disproportionation between one-electron-reduced molecules of Pdr, and oxidation of the fully reduced flavoprotein by artificial electron acceptors, potassium ferricyanide and 2,6-dichlorophenolindophenol (data not shown), proceeded faster at high salt concentrations. This may be due to the effect of ionic strength on intrinsic properties of Pdr, such as protein stability, conformation, flavin environment, and redox potentials, and requires further study.

We also found that NAD^+ affected the electron-accepting and -transferring properties of Pdr and promoted both reduction of Pdr by dRFH$^{\bullet}$ and disproportionation between one-electron-reduced molecules of the flavoprotein (Figure 4). This effect of oxidized pyridine nucleotide on Pdr is different from that on analogous flavoproteins. NAD^+ was found to stabilize the FAD semiquinone of cytochrome b_5 reductase and to appreciably slow its autoxidation and disproportionation (*25*), whereas the rate of disproportionation of adrenodoxin reductase semiquinone was independent of $NADP^+$ (*26*). Oxidized pyridine nucleotides have been demonstrated to play an important role in the catalysis of Pdr and the flavoproteins mentioned above (*12*, *25*−*29*). By specifically affecting the stability of reduced flavin intermediates and their redox potentials, $NAD(P)^+$ is thought to regulate the catalytic cycles of the enzymes and to define which species participate in the catalytic turnover in vivo. Destabilization of the Pdr FAD semiquinone by NAD^+ suggests that the fully reduced species of Pdr is likely to be the predominant form of the flavoprotein that participates in catalysis.

Pdr−Pdx Interaction. Preferential reduction of Pdr by the laser flash in the Pdr−Pdx system gave us an advantage to directly investigate the ET reaction between one-electron-reduced Pdr and oxidized Pdx. Under optimal conditions, a kinetic K_d value for protein−protein transient complex formation was calculated to be 5 μM. The affinity of the Pdx−Pdr ET complex is, therefore, lower than that for the transiently formed complexes between reduced ferredoxin and oxidized ferredoxin reductase [$K_d = 0.3$ μM, (*30*)] and one-electron-reduced cytochrome b_5 reductase and cytochrome b_5 [$K_d = 1$ μM, (*25*)]. The limiting value of k_{obs} for the ET reaction from FADH$^{\bullet}$ of Pdr to Pdx at saturating ratios of Pdx to Pdr was found to be equal to 226 s^{-1}. Taking into account a high intracellular ratio of Pdr to Pdx in *P. putida* [1:8, (*11*)] and a maximal turnover number of the camphor hydroxylation reaction [≈2000 nmol min^{-1} (nmol of P450)$^{-1}$, (*31*)], one can conclude that the ET rates from one-electron-reduced Pdr to Pdx are fast enough to support the turnover of the enzyme under steady-state conditions. FADH$^{\bullet}$ of Pdr, therefore, is a kinetically significant intermediate in the camphor monooxygenation cycle.

The biphasic ionic strength dependence of k_{obs} for ET between Pdr and Pdx (Figure 6B) is similar to that observed with other redox protein systems (*19*, *32*, *33*). The simplest explanation for this behavior is that, at low ionic strengths, either ineffective Pdr−Pdx complexes are being formed or there is an electrostatic repulsion between the proteins. At an ionic strength optimal for the redox partner interaction, there must be a balance between electrostatic attraction and orientation forces as well as hydrophobic interactions between the two proteins. For the Pdr−Pdx redox couple, the maximal ET rates are observed at a relatively high ionic strength. This suggests that nonelectrostatic interactions, such as van der Waals forces, hydrophobic effects, and entropic effects, dominate in Pdr−Pdx complex formation. This conclusion is in accord with the previous site-directed mutagenesis, NMR, and isothermal titration calorimetry studies on Pdr−Pdx interactions that suggested the electrostatic component is not important in Pdx/Pdr association (*7*, *13*, *34*).

Owing to the lack of structural information on Pdr, it is not possible to model an ET complex between Pdr and Pdx. To gain some insights into the structure of Pdr, we have analyzed the crystal structure of a close functional and structural homologue of Pdr, an ONFR component in biphenyl dioxygenase (BphA4) from *Pseudomonas putida* (*15*). There is no strong asymmetric charge distribution on the surface of BphA4. Moreover, the aromatic rings of Trp291, Trp318, and Trp320 and a ring of Pro49 are situated above the isoalloxazine ring of FAD and completely shield from the solvent the side of the flavin that is involved in the reactions. The active site of BphA4, therefore, is mainly neutral with a few negatively and positively charged amino acid residues evenly distributed around. Owing to the high amino acid sequence identity between the FAD binding sites of BphA4 and Pdr, the active site of Pdr is also likely to be mainly neutral and hydrophobic. This speculation could explain some of the results described above. Both the transient kinetics and molecular modeling results suggest that hydrophobic interactions are likely to be predominant in Pdr−Pdx complex formation.

This contrasts the adrenodoxin reductase (Adr)−adrenodoxin (Adx) couple, functional analogues of Pdr and Pdx in mitochondria of eukaryotes, where electrostatic interactions were proved to be the driving force for the interprotein complex formation. Both Adr and Adx are highly polar molecules and have strong dipole moments that are thought to steer the approach and complex formation between the redox partners (*35*−*37*). It is of interest that arecent study

provided evidence that the complex between Adr and Adx does not dissociate to a great extent during an oxidation−reduction cycle, and that 1:1 and 1:2 Adr/Adx complexes exist between protein in the reduced states (*38*). The high affinity of the Adr−Adx complex in both oxidized and reduced states thus supports the cluster model for the interaction between components of the mitochondrial steroid hydroxylase.

Pdx−P450cam Interaction. Although our main goal has been to analyze the Pdr−Pdx ET system, we also analyzed the Pdx-to-P450cam ET reaction. The rate constants for the first electron transfer to P450cam, obtained in the present study (112 s^{-1}), are in a good agreement with those measured previously by different methods under different conditions (30−100 s^{-1}) (*39*−*42*). Our kinetic results support the view that both electrostatic and hydrophobic components are involved in Pdx−P450cam complex formation (*6*, *7*, *13*) but emphasize that electrostatics play a more important role in the association of two proteins. The fact that optimal conditions differ for the Pdr−Pdx and Pdx−P450cam ET reactions supports the view that the binding sites on Pdx for Pdr and P450cam involve different structural elements. Indeed, although some overlap between the binding sites is present, Cys73 and its adjacent α-helix in Pdx were identified as important for the Pdr−Pdx interaction, whereas residues comprising a surface loop subtended by the iron−sulfur cluster were found to be critical for Pdx−P450cam complex formation (*6*, *7*). The precise nature of the association mode of Pdx with its redox partners may be revealed after the structures of the complexes become available.

Finally, our results have implications for the electron shuttle mechanism between all three components. Similar values of K_d's for the transient Pdr−Pdx and Pdx−P450cam ET complexes and the insignificant changes within a wide range of ionic strength indicate that Pdx is not preferably bound to either Pdr or P450cam during the catalytic cycle and is likely to function as an electron shuttle. Indeed, in the complete system containing all three proteins, the maximal turnover number of camphor hydroxylation was observed at an intermediate ionic strength, $I \approx 0.15$ (data not shown). Thus, a balance between specificity in two transient ET complexes involving Pdx is necessary for achieving a rapid exchange of electrons between the redox partners and the maximal turnover number of P450cam monooxygenase.

REFERENCES

1. Mueller, E. J., Loida, P. J., and Sligar, S. G. (1995) in *Cytochrome P450: Structure, Mechanism, and Biochemistry* (Montellano, P. R. O. d., Ed.) 2nd ed., pp 83−125, Plenum Press, New York.
2. Geren, L., Tuls, J., O'Brien, P., Millett, F., and Peterson, J. A. (1986) *J. Biol. Chem. 261*, 15491−15495.
3. Stayton, P. S., and Sligar, S. G. (1990) *Biochemistry 29*, 7381−7386.
4. Davies, M. D., and Sligar, S. G. (1992) *Biochemistry 31*, 11383−11389.
5. Unno, M., Shimada, H., Toba, Y., Makino, R., and Ishimura, Y. (1996) *J. Biol. Chem. 271*, 17869−17874.
6. Holden, M., Mayhew, M., Bunk, D., Roitberg, A., and Vilker, V. (1997) *J. Biol. Chem. 272*, 21720−21725.
7. Aoki, M., Ishimori, K., and Morishima, I. (1998) *Biochim. Biophys. Acta 1386*, 157−167.
8. Pochapsky, T. C., Lyons, T. A., Kazanis, S., Arakaki, T., and Ratnaswamy, G. (1996) *Biochimie 78*, 723−733.
9. Poulos, T. L., Finzel, B. C., and Howard, A. J. (1987) *J. Mol. Biol. 195*, 687−700.
10. Pochapsky, T. C., Ye, X. M., Ratnaswamy, G., and Lyons, T. A. (1994) *Biochemistry 33*, 6424−6432.
11. Roome, P. W., Jr., Philley, J. C., and Peterson, J. A. (1983) *J. Biol. Chem. 258*, 2593−2598.
12. Roome, P. W., and Peterson, J. A. (1988) *Arch. Biochem. Biophys. 266*, 32−40.
13. Aoki, M., Ishimori, K., Fukada, H., Takahashi, K., and Morishima, I. (1998) *Biochim. Biophys. Acta 1384*, 180−188.
14. Roome, P. W., and Peterson, J. A. (1988) *Arch. Biochem. Biophys. 266*, 41−50.
15. Senda, T., Yamada, T., Sakurai, N., Kubota, M., Nashizaki, T., Masai, T., Fukuda, M., and Mitsui, Y. (2000) *J. Mol. Biol. 304*, 397−410.
16. Morales, R., Charon, M.-H., Kachalova, G., Serre, L., Medina, M., Gomez-Moreno, C., and Frey, M. (2000) *EMBO Rep. 1*, 271−276.
17. Kurisu, G., Kusunoki, M., Katoh, E., Yamazaki, T., Teshima, K., Onda, Y., Kimata-Ariga, Y., and Hase, T. (2001) *Nat. Struct. Biol. 8*, 117−121.
18. Susin, S. A., Lorenzo, H. K., Zamzami, N., Marzo, I., Snow, B. E., Brothers, G. M., Mangion, J., Jacotot, E., Costantini, P., Loeffler, M., Larochette, N., Goodlett, D. R., Aebersold, R., Siderovski, D. P., Penninger, J. M., and Kroemer, G. (1999) *Nature 397*, 441−446.
19. Tollin, G., Hurley, J. K., Hazzard, J. T., and Meyer, T. E. (1993) *Biophys. Chem. 48*, 259−279.
20. Tollin, G. (1995) *J. Bioenerg. Biomembr. 27*, 303−309.
21. Gunsalus, I. C., and Wagner, G. C. (1978) *Methods Enzymol. 52*, 166−188.
22. Omura, T., and Sato, R. (1964) *J. Biol. Chem. 239*, 2370−2378.
23. Walker, M. C., Pueyo, J. J., Navarro, J. A., Gomez-Moreno, C., and Tollin, G. (1991) *Arch. Biochem. Biophys. 287*, 351−358.
24. Massey, V., and Palmer, G. (1966) *Biochemistry 5*, 3181−3189.
25. Meyer, T. E., Shirabe, K., Yubisui, T., Takeshita, M., Bes, M. T., Cusanovich, M. A., and Tollin, G. (1995) *Arch. Biochem. Biophys. 318*, 457−464.
26. Kobayashi, K., Miura, S., Miki, M., Ichikawa, Y., and Tagawa, S. (1995) *Biochemistry 34*, 12932−12936.
27. Iyanagi, T. (1977) *Biochemistry 16*, 2725−2730.
28. Kobayashi, K., Iyanagi, T., Ohara, H., and Hayashi, K. (1988) *J. Biol. Chem. 263*, 7493−7499.
29. Lambeth, J. D., and Kamin, H. (1976) *J. Biol. Chem. 251*, 4299−4306.
30. Hurley, J. K., Hazzard, J. T., Martinez-Julvez, M., Medina, M., Gomez-Moreno, C., and Tollin, G. (1999) *Protein Sci. 8*, 1614−1622.
31. Kadkhodayan, S., Coulter, E. D., Maryniak, D. M., Bryson, T. A., and Dawson, J. H. (1995) *J. Biol. Chem. 270*, 28042−28048.
32. Hazzard, J. T., Rong, S. Y., and Tollin, G. (1991) *Biochemistry 30*, 213−222.
33. Hurley, J. K., Fillat, M. F., Gomezmoreno, C., and Tollin, G. (1996) *J. Am. Chem. Soc. 118*, 5526−5531.
34. Aoki, M., Ishimori, K., and Morishima, I. (1998) *Biochim. Biophys. Acta 1386*, 168−178.
35. Ziegler, G. A., Vonrhein, C., Hanukoglu, I., and Schulz, G. E. (1999) *J. Mol. Biol. 289*, 981−990.
36. Muller, A., Muller, J. J., Muller, Y. A., Uhlmann, H., Bernhardt, R., and Heinemann, U. (1998) *Structure 6*, 269−280.
37. Muller, J. J., Lapko, A., Bourenkov, G., Ruckpaul, K., and Heinemann, U. (2001) *J. Biol. Chem. 276*, 2786−2789.

38. Hara, T., Koba, C., Takeshima, M., and Sagara, Y. (2000) *Biochem. Biophys. Res. Commun. 276*, 210−215.
39. Peterson, J. A., and Mock, D. M. (1979) *Acta Biol. Med. Germ. 38*, 153−162.
40. Hintz, M. J., Mock, D. M., Peterson, L. L., Tuttle, K., and Peterson, J. A. (1982) *J. Biol. Chem. 257*, 14324−14332.
41. Brewer, C. B., and Peterson, J. A. (1988) *J. Biol. Chem. 263*, 791−798.
42. Furukawa, Y., and Morishima, I. (2001) *J. Biol. Chem. 276*, 12983−12990.

BI010874D